Small tin oxide grains: structural and electronic properties evaluated using the density functional theory

2007 J. Phys.: Condens. Matter 19 026214

(http://iopscience.iop.org/0953-8984/19/2/026214)

INSTITUTE OF PHYSICS PUBLISHING JOURNAL OF PHYSICS: CONDENSED MATTER

J. Phys.: Condens. Matter **19** (2007) 026214 (11pp) doi:10.1088/0953-8984/19/2/026214

Small tin oxide grains: structural and electronic properties evaluated using the density functional theory

A M Mazzone

CNR-IMM, Sezione di Bologna, Via Gobetti 101, 40129-Bologna, Italy

Received 4 July 2006, in final form 31 October 2006
Published 15 December 2006
Online at stacks.iop.org/JPhysCM/19/026214

Abstract

This study is motivated by the complex properties of tin oxides and by the lack of detailed theoretical information on the clustered state of these materials. Therefore small grains of a columnar and a spherical shape with a rutile lattice and a size up to 100 atoms have been considered and their structural and electronic properties evaluated using the density functional theory. The calculations show that the rutile skeleton is retained starting from a size of 20 atoms and the absence of reconstruction is particularly evident in the spherical grains. However, reconstruction also occurs and the physical force behind it is an increase in the coordination among tin–oxygen and oxygen–oxygen atoms. The binding energy has a primary dependence on the grain size, whereas only marginal effects arise from the grain structure. The density of states has bands below and above the Fermi levels which are not observed in the crystalline material and are therefore peculiar to the clustered state.

(Some figures in this article are in colour only in the electronic version)

1. Introduction

In the field of covalent oxides SnO_2 has both practical and theoretical importance. Much of the interest in this material stems from its value for gas-sensing applications, and to enhance its adsorption capabilities complex structures with porous or ribbon-like geometries are currently being developed. These materials have been the subject of intensive experimental investigation, and accurate characterization, based on TEM and XR techniques, is available for their structural properties (see [1, 2] and references therein). On the theoretical side, efforts have been concentrated on the evaluation of the structure and band properties of the crystalline material and of the most stable of its surfaces, i.e. (110) and (101) (references on both subjects can be found in [3–12] and related works). The adsorption properties, for deposited CO and O_2, have been considered in [13–18] and water adsorption has been described in [19, 20].

However, theoretical studies on the nanocrystalline phase of this material are scarce. Only the stability of nanowires has been analysed, in [21], and that study, in essence, elaborates on the analogy with the surfaces of the crystalline material. The present contribution attempts to fill the gap between the bulk materials considered in the theoretical studies and the complex structures used in experiments. Accordingly, clusters of a spherical and columnar shape with a number of atoms up to 100 have been considered and their properties are evaluated using density functional theory (DFT). The central aim of the calculations is to assess whether these clusters represent a new class of materials or there are traces of the known phases of SnO_2 (for this reason the clusters are also indicated as 'small grains'). The results indicate that the rutile lattice is approximately retained at all sizes and shapes. However, structures with irregular boundaries are stabilized by an increase in the coordination among oxygen and tin atoms. The charge exchanges and hybridization due to this bonding lead to the formation of bands in energy ranges different from those of the bulk material.

2. The computational method

Experimental observations show that the nanocrystalline SnO_2 material, prepared at low temperature, contains units with a linear dimension in the range 10–20 Å formed by clear lattice strings. An increase in the processing temperature leads to the coalescence of these units into grains with dimensions in the range 40–50 Å. Even in those cases the grains and their interfaces retain a good crystalline quality, though defective or amorphous interfaces are also observed (evidence for a rutile structure of the nanocrystalline material is given in [22–25]). Electron microscopy observations show that the plane projection of these grains has an approximately spherical form. However, squared structures, growing from twinning across a nearly perfect interface, are also observed [1, 22, 23]. Furthermore, current technologies lead to the production of nanowires with a squared section and a width–length ratio in the range of many thousands. Despite broad investigations having been performed on the growth techniques, the inherent reasons for the stability of these two types of structures are at present unclear.

The present study is directed at an understanding of the properties of the clustered state of tin oxides and of its evolution towards the macroscopic shapes described above. However, this is not a trivial matter. In fact the potential energy surface of structures of finite size contain a number of local minima which exponentially increases with the size. The evaluation of the most stable structure is complex and in compounds this problem is aggravated by the further degree of freedom arising from their variable composition. The approaches adopted in the literature to circumvent this problem consist of unbiased search algorithms or a search in a group of structures, chosen on the basis of a plausible physical behaviour. For structures of the size and complexity of those considered in this work, the use of mathematical algorithms, which involve a million samplings, is practically unfeasible. On the contrary, a structural analogy with experiments is plausible as the linear dimensions of the structures considered below reach approximately 10 Å and the clusters are therefore only slightly smaller than the spherical grains reported above. Accordingly, the initial cluster structure has a rutile lattice and, in agreement with the spherical and squared structures reported above, clusters with these two shapes (indicated below as 'columnar' and 'spherical') are investigated. These clusters are obtained by cutting a cubic box of the crystalline material parallel to the crystallographic planes of SnO_2 or carving a sphere into this box, and their shape is further refined by minimization of the total energy, using conjugate gradients. The cluster size N spans from approximately 10 to 100 atoms and the ratio between the number of tin and oxygen atoms (indicated below as 'x') varies between 0.43 and 0.57 in the spherical clusters and is constantly equal to 0.5 in the columnar ones. A lattice view of the clusters of the two types is reported in figure 1, and these shapes

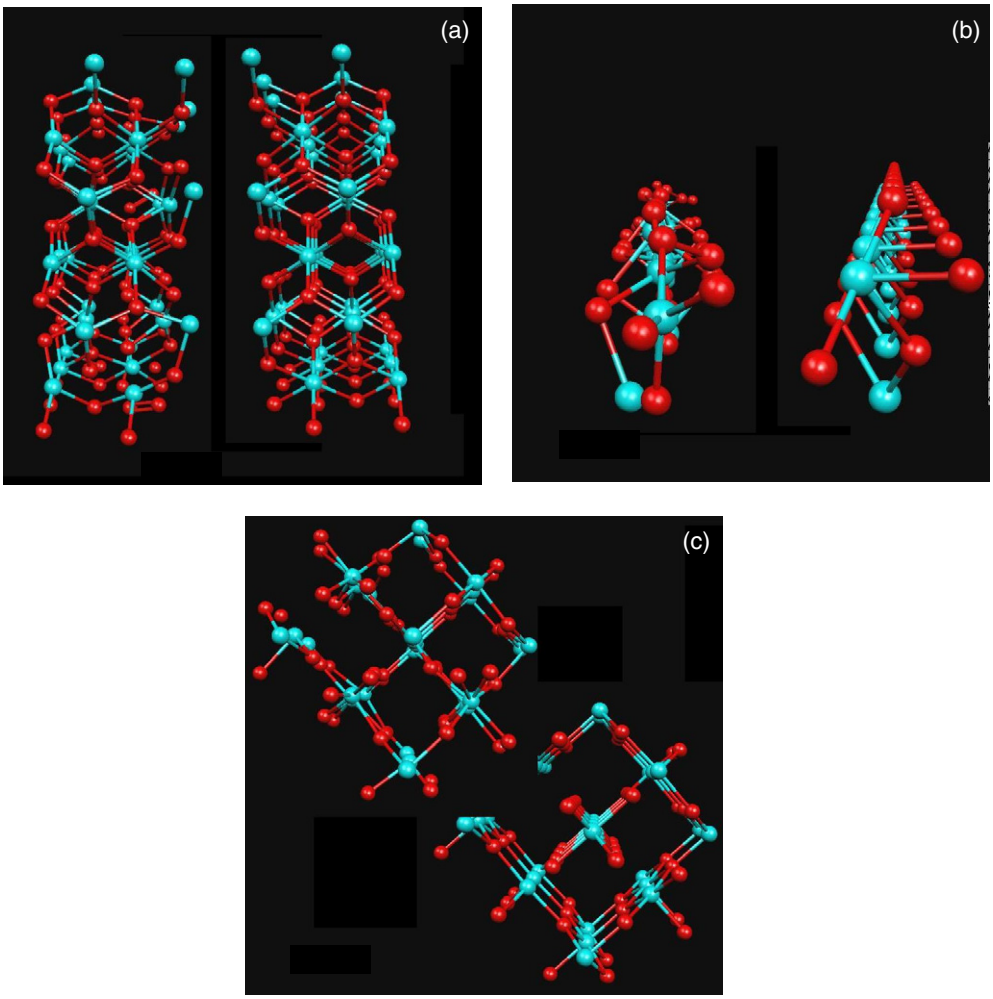

Figure 1. The cluster structure: initial and final stage of the energy minimization. (a), (b) Columnar grains of size $N = 108$ and 48. (c) Spherical grains of size $N = 80$. In (a) and (b) the initial lattice structure is on the right side. In (c) the unreconstructed lattice is partially shown in the insect on the right-hand side. Tin and oxygen atoms are pale (blue) and dark (red), respectively.

will be discussed again below when presenting the properties of the reconstruction. Here we underline only the wirelike structure of the columnar grains with the smaller section illustrated by figure 1(b) and the circular perimeter of the spherical grain presented in figure 1(c). Both features are in agreement with the experimental shapes reported above.

DFT calculations are based on the fully self-consistent pseudopotential method SIESTA [26]. Unless otherwise specified the SIESTA inputs are: a mesh cut-off of 80.0 Ryd, the Troullier–Martins nonlocal pseudopotentials in the Kleinman–Bylander form without or with relativistic corrections (the relativistic corrections are applied only to tin), the Ceperley–Alder correlation functional with the Perdew–Zunger parameterization or the Perdew–Burke–Ernzerhof functional (indicated below as LDA or GGA, respectively; the GGA potential is also used in WIEN97, see below). The electronic configuration of Sn and O is $5s^2 5p^2 4d^{10}$ and $2s^2 2p^4$ with a cut-off radius of the core pseudopotential equal to 1.90 and 1.55 au, respectively.

Table 1. Bulk materials: tin, SnO and SnO_2. Experimental and theoretical evaluation of the cohesive energy.

Cohesive energy of bulk materials			
Material	Structure	Experiments (eV)	Calculations (eV)
α-Sn	—	3.14	3.72(LDA), 2.95(GGA)
β-Sn	—	3.10	3.69(LDA), 2.92(GGA)
SnO	Layered	4.36	5.44(LDA)
SnO_2	Rutile	4.78	5.89(LDA)

The basis sets are formed by Slater-type pseudo atomic orbitals (PAO) constructed from the eigenstates of the atomic pseudopotential. The ones adopted below have either single- or double-ζ quality plus polarization (indicated as $S\zeta$, $D\zeta$, $S\zeta P$, $D\zeta P$, respectively. $D\zeta$ and $D\zeta P$ basis are also used in [15]). The evaluation of the density of states of crystalline SnO_2, reported below, is based on the program WIEN97 [27]. In WIEN97 the wavefunctions are constructed from spherical harmonics with angular momentum up to $l_{max} = 10$ and from plane waves up to an energy cut-off $K^2_{max} = 17$ Ryd. The initial electronic charge is Kr $4d^{10}5s^25p^2$ and He $2s^22p^4$ for tin and oxygen, respectively.

The quantities reported in the following section illustrate the main structural and electronic properties of clusters and have been chosen with the aim of a clear comparison with the bulk material. The structural parameters are the average coordination among different atoms, i.e. c_{av} (tin–tin), c_{av} (oxygen–oxygen), c_{av} (tin–oxygen), the grain volume $dVol$ and the aspect ratio. The coordination c_{av} of tin and oxygen atoms is the average number of atoms of one or other sublattice falling within a distance equal to the bulk value (with a tolerance of 0.4 Å) from the given atom. The cluster volume Vol and the aspect ratio are evaluated from the parallelepiped of the smallest size which envelops the cluster and from the ratio between the inertial moments with respect to two in-plane equatorial axes, respectively ($dVol$ is the volume normalized to the value at the beginning of the relaxation and also the aspect ratio is normalized to its initial value).

The parameters of the electronic configuration are the binding and the Fermi energy, E_b and E_f, respectively, the Mulliken charges (these charges are referred to the valence charge of the neutral atoms) and the density of states (DOS), i.e. DQ_{Sn} and DQ_O. E_f, which indicates the most populated energy levels, is evaluated from the total number of valence electrons, using an unsmeared occupation probability equal to 1. The binding energy E_b has a meaning similar to the cohesive energy of solids (which has, however, the reverse sign) and is the total energy of the system, measured with respect to a system of free atoms. For clusters the DOS calculation is based on an internal utility of SIESTA by grouping the allowed energy levels with an approximately equal E and broadening E by a factor η around 0.5 eV. For crystalline SnO_2 the tetrahedron method [27] has been adopted.

3. Structural and electronic properties of tin oxide clusters

To set the stage briefly, we recall a few properties of stannic oxides. The elements of group IV can, in addition to displaying the +4 oxidation state expected for their group, display an oxidation state of 2 lower, and for Sn this is demonstrated by the occurrence of the two oxides, SnO and SnO_2, and for both oxides the cohesive energy is well above that of pure tin (the energies of all these materials are reported in table 1). In addition, compounds Sn_aO_b, with a broad range of a, b values, depending on the preparation conditions, are also reported in

the technical literature. However, a nanocrystalline phase has been clearly identified only for SnO_2, which has therefore been assumed as the reference state of our clusters. SnO_2 is known to crystallize under ambient conditions in the rutile structure. This lattice has an approximately layered structure with a c/a ratio in the range 0.67. Each tin atom is octahedrally coordinated to four oxygen atoms which are at a distance of 2.06 Å from tin whereas the minimum tin–tin and oxygen–oxygen distances are 2.96 and 2.53 Å, respectively.

The results of the energy optimization are reported in figure 1. The figure illustrates the properties of reconstruction as a function of the cluster size and shape by comparing columnar and spherical clusters of size in the range 80–100 atoms at the beginning and at the end of the energy minimization (the columnar clusters are reported in figures 1(A), (B) and the spherical one in figure 1(C), respectively). In spite of some lattice disorder, the bulk-like structure of the grain skeleton is clearly visible, especially in the spherical cluster. Three elements have to be accounted for to explain the stability of the rutile lattice. First, our own previous study on small clusters of size $N \leqslant 14$ with composition Sn_mO_n [28, 29] showed that two types of structure are energetically possible. In one case the cluster is formed by a skeleton of stable tin clusters into which the oxygen atoms are embedded. However, at the larger sizes, in agreement with the present study, a disordered crystalline fragment was also found to be stable, a result attributed to the large internuclear distances in the rutile lattice. The length of these distances is well above the coordination radius of the two elements (using for this parameter the cut-off of the pseudopotentials or the muffin-tin core radius a value equal to 1.0 and 0.8 Å is obtained for tin and oxygen, respectively) and this prevents effective exchanges and hybridization among lattice atoms. Second, without actually applying an unbiased algorithm, an extensive parametric testing was conducted by slightly modifying the initial shapes into more prolate or oblate forms or by altering the values of the stoichiometric ratio x. All these tests showed results converging to a structure with a rutile lattice. Third, an important justification derives from the properties of the phases of SnO_2 more directly comparable with clusters. One of these phases is obviously the nanocrystalline material. In addition, surface atoms also have a low coordination and experience reconstruction and are therefore similar to cluster atoms. For nanocrystalline SnO_2, x-ray observations, coupled with muffin-tin calculations of the bulk material [25], show a band structure similar that of SnO. This suggests a crystalline structure with undercoordinated surface atoms. Similar features are exhibited by surface atoms. In fact, study of SnO_2 (110) or (101) shows that the relaxation of these surfaces is generally small, within a few per cent of the interlayer spacing in the bulk material, and varies randomly with depth [12]. In the context of this study, these results, on their whole, suggest that a crystalline lattice with reconstructed boundaries is a plausible cluster shape and the main reason for this behaviour is the stability of the Sn_aO_b bonds over a wide range of a, b compositions and internuclear distances.

A detailed analysis of the structural properties of clusters is reported in figures 2 and 3. These figures illustrate the dependence on the cluster size N of $dVol$ and of the aspect ratio (figure 2) and the average coordinations c_{av} (figure 3) for the columnar and spherical structures. Both the aspect ratio and $dVol$ are subtle indicators of the structural properties. In the first place, in fact, they show the deviation of the unit vectors from the a/c ratio in the bulk material and therefore offer a simple estimate of the elastic strain and stresses in the clusters at the potential energy minimum. In the second place $dVol$ amplifies the displacements from the rutile lattice locations adopted at the beginning of the simulation as a relationship $dVol = \mathrm{disp}^3$ approximately holds.

From the plots in figure 2 it is evident that the larger grains preferably retain the initial skeleton as in those cases the asymptotic value of the normalized aspect ratio is 1. These clusters can therefore be regarded as crystalline fragments under both aspects of their structure

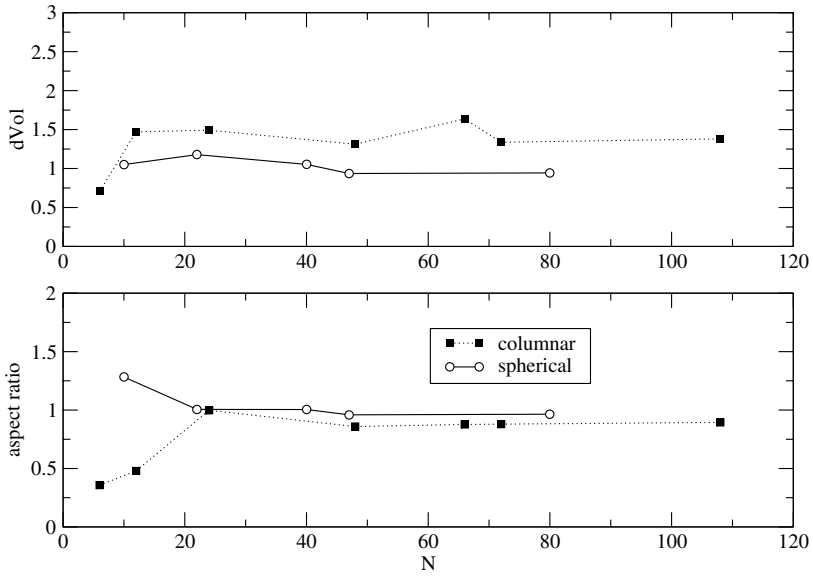

Figure 2. The normalized volume change *dVol* and the aspect ratio as a function of the size *N* for the columnar and spherical clusters.

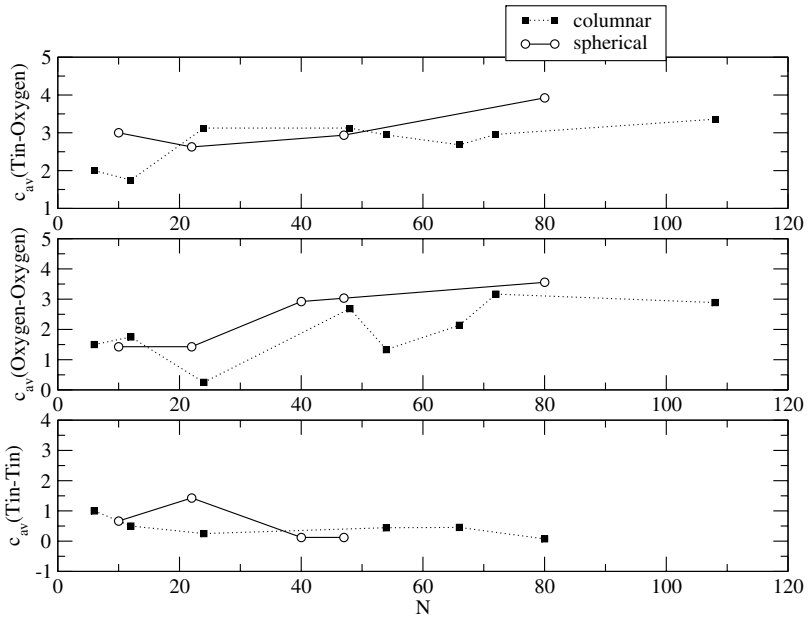

Figure 3. The coordination among tin and oxygen atoms as a function of the size *N* for the columnar and spherical clusters.

and elastic energy. Furthermore the trend towards a limited reconstruction is more evident in the spherical structures than in the columnar ones and the reduced aspect ratio of this last group at the smaller sizes indicates a tendency towards the formation of a spherical shape. In principle, either the cluster composition or its structure may be responsible for these effects. However,

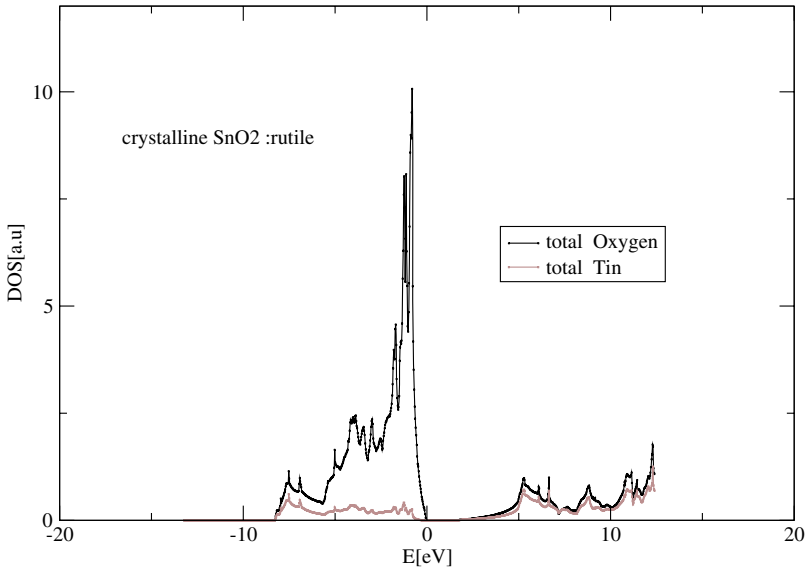

Figure 4. The DOS plot of the crystalline SnO_2 with a rutile lattice. WIEN calculations.

no clear connection was found between the stoichiometric ratio x, on one hand, and the aspect ratio on the other, so that these affects arise from structural properties. As shown by figure 1, disordered rows are preferentially located on the cluster outer mantle, on the cluster edges and on the corners. Owing to the spherical shape, the atoms on the cluster corners are reduced from $N^{1/2}$ in the columnar structures to $N^{1/3}$ in the spherical ones. This property accounts for the shape dependence of the aspect ratio, mentioned above. It also explains the larger values of $dVol$ observed in the columnar grains of larger size.

A noticeable feature of the coordination parameters (figure 3) is that, similarly to $dVol$ and to the aspect ratio, they depend on both the grain structure and its size and that this dependence is different in the two sublattices. Generally, higher c_{av} values are attained in the spherical structures, and this is in agreement with the limited reconstruction observed for these grains. Furthermore in the tin sublattice the trend is towards the increase of the coordination with the oxygen atoms at increasing N whereas the tin–tin coordination is almost constant. On the contrary, in the oxygen sublattice the oxygen–oxygen coordination also increases with N.

The properties of the electronic configuration are illustrated in figures 4–7, which report the DOS, the Mulliken charges and the Fermi and binding energies of the two types of structure (in these calculations different simulation conditions are also analysed). In figures 4 and 5 a comparison is made between the DOS of the bulk material with a rutile lattice and the DOS of clusters of variable size and shape. For the bulk material (figure 4) the DOS plot shows two main bands located across the Fermi energy (assumed as zero in the energy scale). These bands, above and below E_f, are formed by the O 2p and Sn 5p and by the O 2p and Sn 5s states, respectively. A third deeper band, at $E \sim -20$ eV, arising from the Sn d states has been omitted for the sake of clarity in the presentation. These properties are in line with a mixed ionic and covalent type of bonding and in their gross form are also exhibited by the clusters considered in this study. In fact, as shown by figure 5, the DOS plots consist of a main band reaching -10 eV below E_f and a further deeper band located at -22 eV, also observed in the bulk material. However, at variance with this case, a continuum of excited levels above E_f and secondary peaks at energies around -20 eV are observed in clusters of all sizes and shapes.

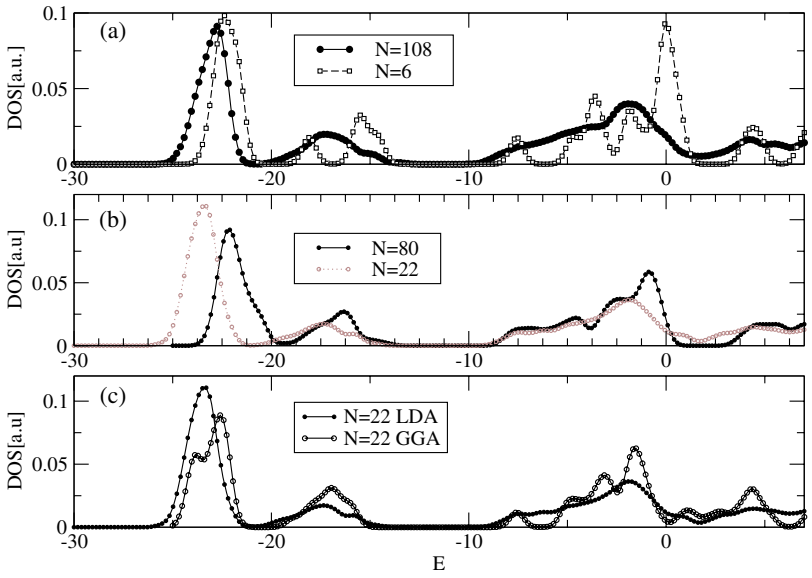

Figure 5. (a) The DOS plot of the columnar clusters of size $N = 108$ and 6. (b) The DOS plot of the spherical cluster $N = 22$ (LDA and $S\zeta$ P). (c) Same as (b) using GGA.

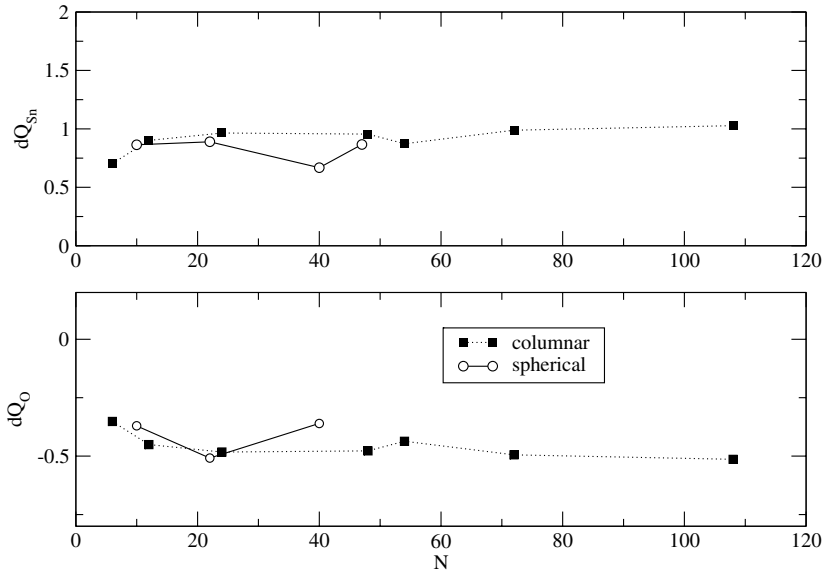

Figure 6. The average Mulliken charge at the bond centre for tin and oygen atoms as a function of the size N for the columnar and spherical clusters.

The projection of DOS on the cluster atoms indicates that these states are produced by orbital mixing due to the increased coordination, as reported above. In addition, size effects are also observed. In fact, the structure of the DOS at small sizes shows separate peaks which are reminiscent of the energy levels of the isolated atom, whereas more compact bands are formed at the larger N.

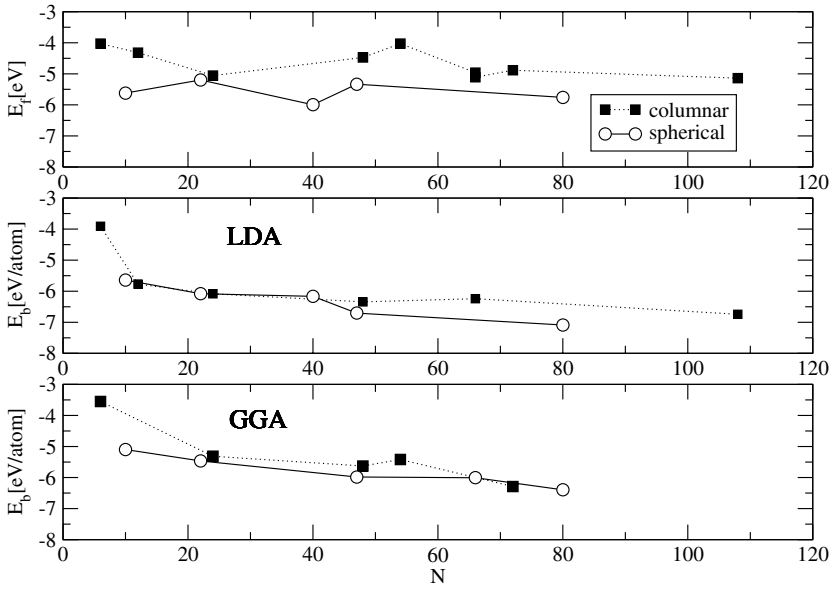

Figure 7. The Fermi and binding energy E_b and E_f as a function of the size N for the columnar and spherical clusters. Calculations using $S\zeta$ P and LDA for E_f. For E_b both LDA and GGA are used.

In previous studies [28, 29] it was shown that for pure tin clusters the value of DQ at the bond centre oscillates around 0.55 and there is also an overlap between second nearest neighbours with a DQ value increasing from 0.16 to 0.27 for increasing values of N. In compound clusters the addition of oxygen atoms leads to similar DQ values for the tin charges whereas the DQ of the oxygen ones are in the range -0.3 and generally the ratio $\mathrm{d}Q_{\mathrm{Sn}}/\mathrm{d}Q_{\mathrm{O}}$ at the bond centre is in close agreement with the stoichiometric ratio x. These charges arise from exchange and hybridization between the s, p and d shells and are one order of magnitude smaller than the bulk ones (in SnO_2 the Mulliken charges are 2.66 and -1.33 for tin and oxygen, respectively [15]) which is the obvious result of the limited interactions in the clusters. Similar values are also observed in the structures considered in this study (figure 6), and in the present context they prove the presence of a covalent component of bonding, which is in agreement with the orbital mixing observed in DOS calculations. It is further underlined that the scarce dependence of these charges on the structural parameters, which is also shared by the DOS and by the characteristic energies, indicates that the effect of the grain shape and size is acts prevalently on the cluster relaxation rather than on its electronic configuration.

The functional relationship between N and the Fermi and binding energies (figure 7) consists of a sharp decrease at the smaller sizes and, starting from $N = 20$, a flat asymptote, a behaviour in agreement with the attainment of a bulk lattice shown by the structural properties. For E_f it is observed that at the smaller sizes this energy has a larger absolute value in the spherical structures than in the columnar ones. In fact, for structures of this last type the stoichiometric ratio x is constantly equal to 0.5 whereas it oscillates between 0.47 and 0.52 in the spherical ones. Therefore the spherical clusters may have a larger tin content than the columnar ones and the lowering of E_f arises from the deep-lying states of tin. However, while at the larger sizes the E_f values of the two types of cluster are indistinguishable, the differences between the values of E_b are perceptible and E_b has larger absolute values in the spherical structures. The effect is attributed to differences between the number of undercoordinated

atoms mentioned above and leads to the interesting conclusion that, while the effects of the composition play a predominant role for E_f, E_b is determined by the cluster structure rather than by its composition.

To conclude, a short note on the computational aspects is in order. A general result of the extensive testing performed on the basis sets and on the potentials needed by the DFT formulation is that the trends described above are qualitatively similar in all cases, though the quantitative differences are significant. The most critical of these divergences are illustrated in the previous figures and tables. The literature results on bulk materials, reported in table 1, show the known LDA overbinding, the amount of which falls in the range 10–20%. A comparison between LDA and GGA calculations of the binding energies and of the DOS is presented in figures 7 and 5. The evaluation of the binding energies (figure 7) shows an increase of E_b in the range 0.5 eV when using GGA. However, in this approach the differences between the columnar and the spherical clusters at the larger sizes are almost inappreciable. This feature would suggest that GGA is less sensitive to the structural properties than LDA. In addition, the comparison of DOS obtained with LDA and GGA (figure 5) shows only marginal changes. Small fluctuations of the electronic parameters, in the range of 10% or less, were found to arise from the basis sets and from pseudopotentials. The structural parameters were found to be stable and their changes were constantly in the range few per cent or less.

4. Conclusions

In conclusion, in this study the structural and electronic properties of clusters of a size only slightly smaller than the grains experimentally observed have been considered. A central result of these calculations is the stability of the rutile lattice. This feature, which is in agreement with experiments, represents an important divergence with respect to the clusters formed by covalent atoms whose shapes significantly deviate from a crystalline fragment. However, reconstruction occurs at all sizes and it takes the form of an increase in the coordination among tin–oxygen and oxygen–oxygen atoms. The analysis of the Mulliken charges indicates charge exchanges and hybridization and the structure of the DOS shows the formation of bands which are not observed in the crystalline material. The spherical grains appear to be more stable than the columnar ones, a result in agreement with the special techniques needed for nanowire fabrication.

References

[1] Parisini A, Angelucci R, Dori L, Poggi A, Maccagnani P, Cardinali G C, Amato G, Lerondel G and Midellino D 2000 *Micron* **31** 223
[2] Comini E, Faglia G, Sberveglier G, Calestani D, Zanotti L and Zha M 2005 *Sensors Actuators* B **111** 2
[3] Peltzer Blanca' E L, Svane A, Christensen N E, Rodriguez C O, Capannini O M and Moreno M S 1993 *Phys. Rev.* B **48** 15712
[4] Meyer M, Onida G, Palummo M and Reining L 2001 *Phys. Rev.* B **64** 45119
[5] Cox D F, Fryberger T B and Semancik S 1988 *Phys. Rev.* B **38** 2072
[6] Godin T J and LaFemina J P 1995 *Phys. Rev.* B **47** 6518
[7] Goniakowski J, Holender J M, Kantorovich L N, Gillan M J and White J A 1996 *Phys. Rev.* B **53** 957
[8] Manassidis I, Goniatowski J, Kantorovich L N and Gillan M J 1995 *Surf. Sci.* **339** 258
[9] Maki-Jaskari M A and Rantala T T 2001 *Phys. Rev.* B **64** 75407
[10] Rantala T T, Rantala T S and Lantto V 2001 *Mater. Sci. Semicond. Process.* **3** 130
[11] Oviedo J and Gillan M J 2002 *Surf. Sci.* **513** 26
[12] Bergermayer W and Tanaka I 2004 *Appl. Phys. Lett.* **84** 99
[13] Goniakowski J and Gillan M J 1996 *Surf. Sci.* **350** 145
[14] Calatayud M, Andres J and Beltran A 1999 *Surf. Sci.* **430** 213
[15] Melle-Franco M and Pacchioni G 2000 *Surf. Sci.* **461** 54

[16] Rantala T T, Rantala T S and Lantto V 2000 *Sensors Actuators* B **65** 375
[17] Sensato F R, Custodio R, Calatayud M, Beltran A, Andres J, Sambrano J R and Longo E 2002 *Surf. Sci.* **511** 402
[18] Yamaguchi Y, Nagasawa Y, Shimomura S, Tabata K and Suzuki E 2000 *Chem. Phys. Lett.* **316** 477
[19] Gercher V A and Cox D F 1994 *Chem. Phys. Lett.* **322** 177
[20] Lindan P J D 2000 *Chem. Phys. Lett.* **328** 325
[21] Dai Z R, Pan Z W and Wang Z L 2002 *J. Phys. Chem.* **106** 302
[22] Dazhi W, Shulin W, Jun C, Suyan Z and Fangqing L 1994 *Phys. Rev.* B **49** 14282
[23] Yu K M, Xiong Y, Lio Y and Xiong C 1997 *Phys. Rev.* B **66** 2666
[24] Launay M, Boucher F and Moreau P 2004 *Phys. Rev.* B **69** 35101
[25] Kucheyev S O, Bauman T F, Stern P A, Wang Y M, van Bureen T, Hanza A V, Terminello L J and Wiley T M 2005 *Phys. Rev.* B **72** 35404
[26] Soler J M, Artacho E, Gale J D, Garcia A, Junquera J, Ordejon P and Sanchez-Portal D 2002 *J. Phys.: Condens. Matter* **14** 2745
[27] Blaha P, Schwarz K and Luitz J 1999 *WIEN97—A Full Potential Linearized Augmented Plane Wave Package for Calculating Crystal Properties* ed K Schwarz (Austria: Tech. Universität Wien) ISBN, 3-9501031-0-4
[28] Mazzone A M 2001 *Comput. Mater. Sci.* **21** 211
Mazzone A M 2002 *Phil. Mag. Lett.* **82** 99
Mazzone A M 2004 *Phil. Mag. Lett.* **84** 275
[29] Mazzone A M and Morandi V 2006 *Eur. Phys. J.* B published on line
[30] Nagase S 1993 *Pure Appl. Chem.* **65** 675